ISSN 0021-3640, JETP Letters, 2021, Vol. 113, No. 1, pp. 47–51. © Pleiades Publishing, Inc., 2021.
Russian Text © The Author(s), 2021, published in Pis'ma v Zhurnal Eksperimental'noi i Teoreticheskoi Fiziki, 2021, Vol. 113, No. 1, pp. 52–57.

CONDENSED MATTER

Tunneling Relaxation Mechanisms of the Jahn–Teller Complexes in a $CaF_2:Cr^{2+}$ Crystal

M. N. Sarychev[a], A. S. Bondarevskaya[a], I. V. Zhevstovskikh[a, b], V. A. Ulanov[c, d], G. S. Shakurov[d], A. V. Egranov[e, f], V. T. Surikov[g], N. S. Averkiev[h], and V. V. Gudkov[a, i, *]

[a] *Institute of Physics and Technology, Ural Federal University, Yekaterinburg, 620002 Russia*
[b] *Institute of Metal Physics, Ural Branch, Russian Academy of Sciences, Yekaterinburg, 620137 Russia*
[c] *Kazan State Power Engineering University, Kazan, 420066 Russia*
[d] *Zavoisky Physical-Technical Institute, FRC Kazan Scientific Center, Russian Academy of Sciences, Kazan, 420029 Russia*
[e] *Vinogradov Institute of Geochemistry and Analytical Chemistry, Siberian Branch, Russian Academy of Sciences, Irkutsk, 664033 Russia*
[f] *Irkutsk State University, Irkutsk, 664003 Russia*
[g] *Institute of Solid State Chemistry, Ural Branch, Russian Academy of Sciences, Yekaterinburg, 620990 Russia*
[h] *Ioffe Institute, Russian Academy of Sciences, St. Petersburg, 194021 Russia*
[i] *South Ural State University, Chelyabinsk, 454080 Russia*
**e-mail: v.v.gudkov@urfu.ru*

Received October 29, 2020; revised November 20, 2020; accepted November 21, 2020

The temperature dependences of attenuation and the velocity of ultrasonic waves at frequencies of 26–158 MHz in a CaF_2 fluorite crystal at the substitution of Jahn–Teller Cr^{2+} centers for calcium ions have been studied. An abnormally high relaxation rate, which is two orders of magnitude higher than the relaxation rate in other previously studied $CaF_2:Ni^{2+}$ and $SrF_2:Cr^{2+}$ fluorites, has been found in the system of Jahn–Teller complexes in the low-temperature region. It has been shown that the global minima of the adiabatic potential energy surface of the $Cr^{2+}F_8^-$ complexes in the $CaF_2:Cr^{2+}$ crystal also have orthorhombic symmetry but are separated by significantly lower potential energy barriers than in $CaF_2:Ni^{2+}$ and $SrF_2:Cr^{2+}$ crystals. It has been found that tunneling relaxation mechanisms (direct and two-phonon transitions) are dominant, rather than thermal activation, in $CaF_2:Cr^{2+}$ in the temperature range where the Jahn–Teller effect is manifested in an ultrasonic experiment. The parameters characterizing these relaxation mechanisms have been determined.

DOI: 10.1134/S0021364021010082

The Jahn–Teller (JT) effect [1] has a significant impact on the structure and physical properties of polyatomic systems. It is considered (or analogies are found in the description) in the course of studies of multiferroics [2–4], fullerenes [5, 6], magnets [7], superconductors [8], perovskites [9, 10], bilayer graphenes [11], and other systems [12, 13]. In solids, the Jahn–Teller effect can be manifested in two versions: as a cooperative effect, where Jahn–Teller centers are embedded in the crystal lattice, or be observed in a system of noninteracting JT complexes formed by vacancies or low-concentration impurities. In the latter case, crystals with the substitution of $3d$ ions for cations are most often studied. Doped crystals are mainly studied by optical or magnetic resonance methods [14–19]. This is due, on one hand, to their application in optoelectronics and spintronics and, on the other hand, to the presence of experimental complexes for such studies produced by well-known firms. Ultrasound studies in the frequency range about 10^8 Hz and higher are performed on single original setups, and therefore the number of such works is much less. At the same time, they make it possible to obtain information about the objects under study that is not available by other methods. Recently, the methods have been developed that make it possible to use ultrasonic experimental data to determine the symmetry properties of the extrema of the lower sheet of the adiabatic potential energy surface (APES) of JT complexes, vibronic coupling constants (linear and quadratic), and positions of extrema in the system of symmetrized coordinates, as well as to study the dynamic properties of JT complexes: relaxation times

and the relaxation mechanisms defining them in cubic [20, 21] and hexagonal crystals [22].

One of the most studied $3d$ ions is Cr^{2+}. It has the ${}^5T_2(t_2^2e^2)$ orbital term in the tetrahedral and cubic coordination (see Table 1 in [14]). According to the EPR data, the global APES minima of Cr^{2+} centers have tetragonal symmetry in the tetrahedral coordination [23–26] and orthorhombic or tetragonal symmetry in the cubic coordination [17, 18, 27–31].

Jahn–Teller Cr^{2+} centers were studied in ZnSe [32], CdSe [22], and SrF_2 matrices using the ultrasonic method [33, 34]. The APES parameters and the vibronic coupling constants were determined in these crystals, and the temperature dependences of the relaxation time were plotted. In addition, it was established that the dominant relaxation mechanism is thermal activation in the region of the attenuation and ultrasound velocity anomalies associated with the manifestation of the JT effect. It was also shown that tunneling mechanisms (direct and two-phonon transitions) are switched on at low temperatures; however, reliable quantitative data characterizing these mechanisms could not be obtained because of their small contribution far from the JT anomalies, i.e., in the region $\omega\tau \gg 1$ (ω is the circular frequency of the ultrasonic wave and τ is the relaxation time of the system of JT complexes).

Since the relaxation processes of the $Cr^{2+}F_8^-$ complex in the CaF_2 matrix have not yet been studied, we measured the temperature dependences of the attenuation coefficient and phase velocity of all normal modes propagating in the [110] direction in the CaF_2:Cr^{2+} crystal with the chromium impurity concentration $n = 4.74 \times 10^{-19}$ cm^{-3} at frequencies of 26–158 MHz.

The measurement results were unexpected: the anomalies associated with the JT effect in this crystal appeared at much lower temperatures than in other studied fluorites SrF_2:Cr^{2+} [34] and CaF_2:Ni^{2+} [21]. Thus, *a unique opportunity has emerged for the quantitative study of tunneling relaxation mechanisms*. However, new difficulties arose: the previously used method [20] for constructing the temperature dependence of the relaxation time $\tau(T)$ turned out to be inapplicable because of the uncertainty of the low-temperature attenuation limit and the ultrasound velocity (it can be seen in Fig. 1 that it is impossible to determine the values of curves *1* and *2* in the limit $T \to 0$). These values are necessary to determine the relaxation contributions, which are used to calculate the temperature dependence of the relaxation time. For this reason, we developed a new approach to an ultrasonic experiment and data processing in the study of the JT effect; this approach allowed the first study of tunneling relaxation mechanisms of JT complexes in the CaF_2:Cr^{2+} fluorite crystal as an example.

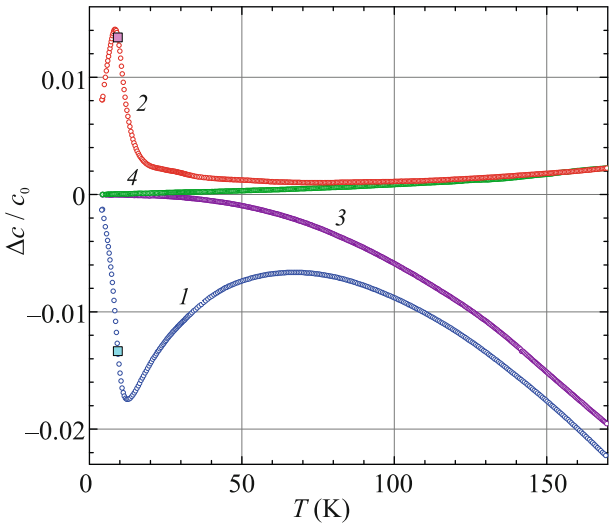

Fig. 1. (Color online) Temperature dependences of the (curves *1* and *3*) real and (*2* and *4*) imaginary parts of $\Delta c/c_0 = c(T)/c_0 - 1$, where $c(T) = c_L = (c_{11} + c_{12} + 2c_{44})/2$ is the elastic modulus measured at a frequency of $\omega/2\pi$ = 54 MHz and $c_0 = c(T \to 0)$. Curves *1* and *2* refer to the doped CaF_2:Cr^{2+} crystal, whereas curves *3* and *4* correspond to nominally pure CaF_2. Squares correspond to the modulus values at the temperature $T = T_1$, at which $\omega\tau = 1$.

Our consideration assumes the description of the space and time dependences of oscillating variables as $\exp[i(\omega t - \mathbf{k}\cdot\mathbf{r})]$; in this case, the complex wave vector is defined as $\mathbf{k} = (\omega/v - i\alpha)\mathbf{e}_k$. It is more convenient to conduct further discussion in terms of dynamic (frequency-dependent) complex elastic moduli c, whose changes are associated with changes in the phase velocity v and attenuation coefficient α of normal modes as follows [20]:

$$\frac{\Delta c}{c_0} = 2\left(\frac{\Delta v}{v_0} + i\frac{\Delta\alpha}{k_0}\right), \qquad (1)$$

where $k_0 = \omega/v_0$, $v_0 = v(T_0)$, $\Delta v = v(T) - v_0$, $\Delta c = c(T) - c_0$, $c_0 = c(T_0)$, $\Delta\alpha = \alpha(T) - \alpha_0$, $\alpha_0 = \alpha(T_0)$, and T_0 is a fixed temperature. The relaxation contribution to the dynamic elastic modulus, in our case the JT contribution Δc_{JT}, is described using the isothermal modulus c_{JT}^T and time dispersion factor $\omega\tau$:

$$\frac{\Delta c_{JT}}{c_0} = \frac{c_{JT}^T}{c_0}\left[\frac{1 - i\omega\tau}{1 + (\omega\tau)^2}\right]. \qquad (2)$$

We studied the tetragonal ($c_E = (c_{11} - c_{12})/2$), trigonal ($c_T = c_{44}$), and longitudinal ($c_L = (c_{11} + c_{12} + 2c_{44})/2$) elastic moduli. These moduli in the above formulas are associated with transverse, polarized along the [–110] and [001] axes, and longitudinal

modes propagating along the [110] crystallographic axis, respectively. The contribution of the JT subsystem to the elastic moduli is manifested as a peak in the imaginary part and a minimum in the real part in the temperature range $T \approx T_1$ (T_1 satisfies the condition $\omega\tau(T_1) = 1$). We note that isothermal moduli are inversely proportional to temperature (see, e.g., [14]); therefore, the position of the relaxation attenuation peak, strictly speaking, does not coincide with T_1, but the T_1 value can be determined by the maximum of the function $f(T) = \mathrm{Im}[\Delta c_{JT}(T)]T/c_0$ or zero of its derivative df/dT. In view of this circumstance, Eq. (2) can be represented in the form

$$\frac{\Delta c_{JT}}{c_0} = 2\frac{\mathrm{Re}[\Delta c_{JT}(T_1)]}{c_0}\frac{T_1}{T}\frac{1}{1+(\omega\tau)^2} + i2\frac{\mathrm{Im}[\Delta c_{JT}(T_1)]}{c_0}\frac{T_1}{T}\frac{\omega\tau}{1+(\omega\tau)^2}. \quad (3)$$

To obtain the JT (relaxation) contribution to the imaginary part of the elastic modulus, it was assumed in previous works (see, e.g., [21]) that the background modulus (the contribution of mechanisms other than the JT effect) can be represented as a monotonic function coinciding with that measured at high ($T \gg T_1$) and low ($T \ll T_1$) temperatures. Obviously, this approach can be applied if the attenuation relaxation peak is well resolved. However, it occurred that the low-temperature limit was not reached in the CaF_2:Cr^{2+} crystal and the attenuation relaxation peak was not fully measured at $T \ll T_1$. Figure 1 shows the temperature dependences of the relative changes in the real and imaginary parts of the modulus c_L obtained at a frequency of 54 MHz (curves *1* and *2*). Qualitatively similar dependences were obtained for all studied moduli. The determination of the relaxation contribution required the measurement of the real and imaginary parts of the moduli on a nominally pure CaF_2 crystal (see curves *3* and *4* in Fig. 1). The relaxation contribution to the imaginary part of the modulus was determined under the assumption that this contribution at high temperatures (in our case, above 170 K) tends to zero because of a small value of $\omega\tau$ and proportionality of the isothermal modulus to the inverse temperature $1/T$, and the contribution to the real part of the modulus is obtained from the condition $\mathrm{Re}\,\Delta c_{JT}(T_1) = -\mathrm{Im}\,c_{JT}(T_1)$. The temperature dependences of the relaxation time $\tau(T)$ calculated by the expression [20]

$$\tau = \frac{1}{\omega}\frac{\mathrm{Im}\,\Delta c_{JT}(T_1)T_1}{\mathrm{Im}\,\Delta c_{JT}(T)T} \pm \frac{1}{\omega}\sqrt{\left[\frac{\mathrm{Im}\,\Delta c_{JT}(T_1)T_1}{\mathrm{Im}\,\Delta c_{JT}(T)T}\right]^2 - 1} \quad (4)$$

for different moduli and different frequencies coincided in the temperature range below 10 K, as it should be, and did not coincide at higher temperatures (Fig. 2, curves *1* and *2*). Moreover, they turned out to be nonmonotonic functions.

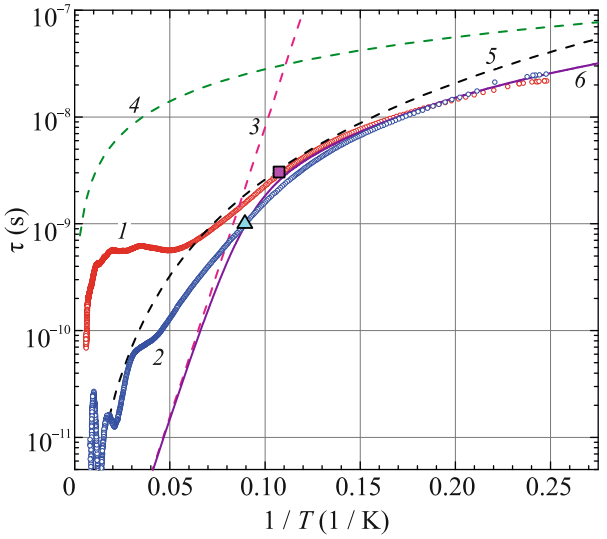

Fig. 2. (Color online) Relaxation time versus the inverse temperature. Curves *1* and *2* are calculated by Eq. (4) with the experimental data on the imaginary parts of the elastic modulus $c_L = (c_{11} + c_{12} + 2c_{44})/2$ for a frequency of (*1*) 54 and (*2*) 158 MHz. Curve *3* is the relaxation time calculated by the formula $\tau_a = 0.3\times10^{-13}\exp(125/T)$, curve *4* is $\tau_t = 2.8\times10^{-7}T^{-1}$, curve *5* is $\tau_R = 2.6\times10^{-6}T^{-3}$, and curve *6* is $\tau = (\tau_a^{-1} + \tau_t^{-1} + \tau_R^{-1})^{-1}$. The square and the triangle correspond to $\tau(T_1^{-1})$ for a frequency of 54 and 158 MHz, respectively.

A significant difference in relaxation times at temperatures above 10 K for frequencies of 54 and 158 MHz (curves *1* and 2 in Fig. 2) can be due to the presence of other subsystems experiencing relaxation. Figure 1 shows that the dependence of the imaginary part of the elastic modulus in the CaF_2:Cr^{2+} crystal (curve *2*) has a "shoulder" in the temperature range near 20 K, apparently due to one or more relaxation contributions, while Eq. (4) was obtained under the assumption that only one relaxing subsystem is present. The analysis of the composition of the crystal studied using an ELAN 9000 ICP-MS (PerkinElmer SCIEX) instrument showed that there is only one impurity comparable to chromium in concentration, namely, an iron impurity (its concentration was 3.45×10^{18} cm^{-3}). However, the isovalent substitution of iron for calcium would lead to the $E \otimes e$ problem of the JT effect, i.e., to the tetragonal distortions of the complex, and, as a consequence, to the absence of anomalies in the trigonal modulus c_{44}. Jahn–Teller anomalies are observed in all moduli in our experiments. Thus, the global APES minima have orthorhombic symmetry, which is possible only in the case of the T term. The shoulder on curve *2* (Fig. 1) is possibly due to the

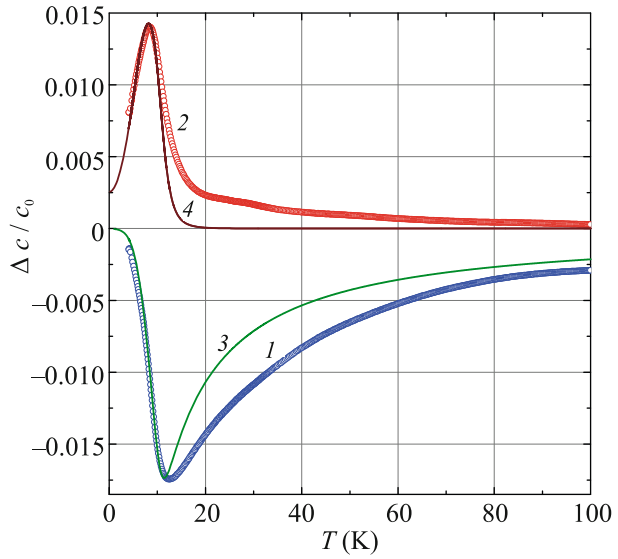

Fig. 3. (Color online) Temperature dependences of the relaxation JT contribution to the (*1*) real and (*2*) imaginary parts of $\Delta c/c_0 = c(T)/c_0 - 1$, where $c(T) = c_L = (c_{11} + c_{12} + 2c_{44})/2$ is the elastic modulus measured at the frequency $\omega/2\pi$ = 54 MHz and $c_0 = c(T = 170$ K). Curves *3* and *4* are model dependences calculated by Eq. (3) with the relaxation time shown by curve *6* in Fig. 2.

presence of Cr^{3+} ions or vacancies with triple degenerate orbital states, which can lead to anomalies in elastic moduli caused by the JT effect. Therefore, it was required to determine the true temperature dependence of the relaxation time of the system of JT $Cr^{2+}F_8^-$ complexes in the CaF_2 matrix.

To this end, we simulated the temperature dependence of the relaxation time taking into account three mechanisms: thermal activation $\tau_a = \tau_0 \exp(V_0/T)$, direct $\tau_t = (BT)^{-1}$ and two-phonon $\tau_R = (B\Theta^2)^{-1}T^{-3}$ tunneling transitions. The consideration of these mechanisms was proposed by Sturge [14] in the first ultrasound studies of the JT effect. The criterion for the correct selection of the parameters appearing in the expressions for different mechanisms of the relaxation time was the coincidence of the model, calculated using Eq. (3), and the experimental temperature dependences of the real and imaginary parts of all measured elastic moduli in the temperature range below 10 K for all measured frequencies: c_L (26, 54, and 158 MHz), c_{44} (39 MHz), and c_E (55 MHz). Thus, the description of $\tau(T)$ should be not only qualitative but also quantitatively unified for all ten measured curves. An example of model curves for the modulus c_L obtained at a frequency of 54 MHz is given in Fig. 3 (curves *3* and *4*). During the simulation, the activation mechanism was always described by the relaxation time $\tau_a = 3\times10^{-14}\exp(125/T)$, and other parameters were in the intervals of $B^{-1} = (2.9–3.3)\times10^{-7}$ s K and $(B\Theta^2)^{-1} = (2.4–2.6)\times10^{-6}$ s K^3. The error in determining the parameters of tunneling relaxation mechanisms did not exceed 10%. This is undoubtedly a good result, especially because tunneling relaxation mechanisms formed only the low-temperature wings of anomalies and their parameters could not be established in previous studies with good accuracy because of a small contribution to the elastic moduli. The estimate $V_0 = 125$ K is due to the following: at a lower activation energy V_0, the predominant relaxation mechanisms would become tunneling mechanisms not only in the low-temperature region but also at $T \gg T_1$, which is physically unreal, and at $V_0 > 125$ K, JT anomalies would be shifted to the region of higher temperatures than is observed in the experiment.

To summarize, the study of the propagation of ultrasonic waves at frequencies of 26–158 MHz in the $CaF_2:Cr^{2+}$ crystal at low temperatures, where tunneling relaxation mechanisms dominate, has revealed for the first time an anomalously high relaxation rate, two orders of magnitude higher than the relaxation rate in other previously studied JT complexes. A new method has been developed to plot the temperature dependence of the relaxation time for the dominant subsystem. It is based on the simulation of the temperature dependences of the real and imaginary parts of the elastic moduli taking into account the activation and tunneling relaxation mechanisms. Parameters that characterize the relaxation times of the JT subsystem caused by direct tunneling transitions and two-phonon transitions have been determined for the first time: $B^{-1} = (3.1 \pm 0.2)\times10^{-7}$ s K and $(B\Theta^2)^{-1} = (2.5 \pm 0.1)\times10^{-6}$ s K^3, respectively. The tunneling relaxation mechanisms in the $CaF_2:Cr^{2+}$ crystal turned out to be dominant, since the activation energy determining the potential energy barrier was significantly lower (V_0 = 125 K = 87 cm^{-1}) than that in other fluorites, where this parameter was 390 K = 271 cm^{-1} for $SrF_2:Cr^{2+}$ [34] and 570 K = 396 cm^{-1} for $CaF_2:Ni^{2+}$ [21].

FUNDING

The work at the Ural Federal University was supported by the Russian Foundation for Basic Research (project no. 18-02-00332a); by the Center of Excellence "Radiation and Nuclear Technologies," Ural Federal University; and by the Ministry of Science and Higher Education of the Russian Federation (state task no. FEUZ-2020-0060). The work at the South Ural State University was supported by the Government of the Russian Federation (act no. 211, contract no. 02.A03.21.0011, project 5-100). The study at the Institute of Metal Physics, Ural Branch, Russian Academy of Sciences, was supported by the Ministry of Science and Higher Education of the Russian Federation (state task no. AAAA-A18-118020190098-5).

REFERENCES

1. H. A. Jahn and E. Teller, Proc. R. Soc. A **161**, 220 (1937).
2. I. B. Bersuker, J. Phys.: Conf. Ser. **833**, 012001 (2017).
3. M. Acosta, N. Novak, V. Rojas, S. Patel, R. Vaish, J. Koruza, G. A. Rossetti, and J. Rödel, Appl. Phys. Rev. **4**, 041305 (2017).
4. M. D. Kaplan and G. O. Zimmerman, J. Phys.: Conf. Ser. **833**, 012007 (2017).
5. D. Liu, N. Iwahara, and L. F. Chibotaru, Phys. Rev. B **97**, 115412 (2019).
6. J. L. Dunn and E. Rashed, J. Phys.: Conf. Ser. **1148**, 012003 (2018).
7. Yu. S. Orlov, S. V. Nikolaev, S. G. Ovchinnikov, and A. I. Nesterov, JETP Lett. **112**, 250 (2020).
8. H. Koizumi, J. Phys.: Conf. Ser. **833**, 012016 (2017).
9. S. Merten, O. Shapoval, B. Damaschke, K. Samwer, and V. Moshnyaga, Sci. Rep. **9**, 2387 (2019).
10. V. Polinger and I. B. Bersuker, J. Phys.: Conf. Ser. **833**, 012012 (2017).
11. M. Angeli, E. Tosatti, and M. Fabrizio, Phys. Rev. X **9**, 041010 (2019).
12. A. V. Kuzmin, S. S. Khasanov, K. P. Meletov, and R. P. Shibaeva, J. Exp. Theor. Phys. **128**, 878 (2019).
13. K. M. Krasikov, A. N. Azarevich, V. V. Glushkov, A. L. Khoroshilov, A. V. Bogach, N. Yu. Shitsevalova, V. B. Filippov, and N. E. Sluchanko, JETP Lett. **112**, 413 (2020).
14. M. D. Sturge, *The Jahn–Teller Effect in Solids,* Vol. 20 of *Solid State Physics,* Ed. by F. Seitz, D. Turnbull, and H. Ehrenreich (Academic, New York, London, 1968), p. 91.
15. W. Ulrici, Phys. Status Solidi **84**, K155 (1977).
16. M. M. Zaripov, V. F. Tarasov, V. A. Ulanov, G. S. Shakurov, and M. L. Popov, Phys. Solid State **37**, 437 (1995).
17. P. B. Oliete, V. M. Orera, and P. J. Alonso, Phys. Rev. B **53**, 3047 (1996).
18. P. B. Oliete, V. M. Orera, and P. J. Alonso, Phys. Rev. B **54**, 12099 (1996).
19. S. K. Hoffmann, J. Goslar, S. Lijewski, and V. A. Ulanov, J. Chem. Phys. **127**, 124705 (2007).
20. V. V. Gudkov, in *The Jahn–Teller Effect: Fundamentals and Implications for Physics and Chemistry,* Ed. by H. Koppel, D. R. Yarkony, and H. Barentzen (Springer, Berlin, Heidelberg, 2009), p. 743.
21. M. N. Sarychev, W. A. L. Hosseny, A. S. Bondarevskaya, I. V. Zhevstovskikh, A. V. Egranov, O. S. Grunskiy, V. T. Surikov, N. S. Averkiev, and V. V. Gudkov, J. Alloys Compd. **848**, 156167 (2020).
22. N. S. Averkiev, I. B. Bersuker, V. V. Gudkov, I. V. Zhevstovskikh, M. N. Sarychev, S. Zherlitsyn, S. Yasin, Yu. V. Korostelin, and V. T. Surikov, J. Exp. Theor. Phys. **129**, 72 (2019).
23. J. J. Krebs and G. H. Stauss, Phys. Rev. B **16**, 971 (1977).
24. G. H. Stauss, J. J. Krebbs, and R. L. Henry, Phys. Rev. B **16**, 974 (1977).
25. J. T. Vallin and G. T. Watkins, Phys. Rev. B **9**, 2051 (1974).
26. J. Dziesiaty, P. Peka, M. U. Lehr, A. Klimakow, S. Muller, and H.-J. Schulz, Z. Phys. Chem. **201**, 63 (1997).
27. M. M. Zaripov, V. F. Tarasov, V. A. Ulanov, G. S. Shakurov, and M. L. Popov, Phys. Solid State **37**, 437 (1995).
28. M. M. Zaripov, V. F. Tarasov, V. A. Ulanov, and G. S. Shakurov, Phys. Solid State **38**, 249 (1996).
29. M. M. Zaripov, V. F. Tarasov, V. A. Ulanov, and G. S. Shakurov, Phys. Solid State **44**, 2050 (2002).
30. P. B. Oliete, V. M. Orera, and P. J. Alonso, J. Phys.: Condens. Matter **8**, 6797 (1996).
31. P. B. Oliete, C. A. Bates, and J. L. Dunn, J. Phys.: Condens. Matter **11**, 2579 (1999).
32. V. V. Gudkov, I. B. Bersuker, I. V. Zhevstovskikh, Yu. V. Korostelin, and A. I. Landman, J. Phys.: Condens. Matter **23**, 115401 (2011).
33. N. S. Averkiev, I. B. Bersuker, V. V. Gudkov, I. V. Zhevstovskikh, M. N. Sarychev, S. Zherllitsyn, S. Yasin, G. S. Shakurov, V. A. Ulanov, and V. T. Surikov, in *Fluorite: Structure, Chemistry and Applications,* Ed. by M. van Asten (Nova Science, New York, 2019), Chap. 2, p. 111.
34. I. V. Zhevstovskikh, I. B. Bersuker, V. V. Gudkov, N. S. Averkiev, M. N. Sarychev, S. Zherlitsyn, S. Yasin, G. S. Shakurov, V. A. Ulanov, and V. T. Surikov, J. Appl. Phys. **119**, 225108 (2016).

Translated by L. Mosina